Fuel 197 (2017) 459–466

Contents lists available at ScienceDirect

Fuel

journal homepage: www.elsevier.com/locate/fuel

Combustion of ligaments and droplets expelled after the end of injection in a multi-hole diesel injector

Radboud Pos [a,*], Madan Avulapati [a], Robert Wardle [b], Roger Cracknell [b], Thanos Megaritis [a], Lionel Ganippa [a]

[a] Brunel University, College of Engineering, Design and Physical Sciences, Uxbridge UB8 3PH, United Kingdom
[b] Shell Global Solutions, Brabazon House, Threapwood Road, Concord Business Park, Manchester M22 0RR, United Kingdom

HIGHLIGHTS

- Both new and used injectors expel liquid fuel post-injection in a random manner.
- The amount of fuel expelled is independent of injector age/mileage.
- The expelled ligaments and droplets remained visible up to 25 ms after EOI.
- In a constant volume chamber these expulsions will continue combustion long after EOI.

ARTICLE INFO

Article history:
Received 4 November 2016
Received in revised form 3 February 2017
Accepted 14 February 2017

Keywords:
Diesel sprays
Common-rail injectors
Post injection expulsions
Post injection ligaments and droplets
Engine-out soot
Combustion

ABSTRACT

Experimental investigations were carried out to study the end of injection spray characteristics using a number of multi-hole common-rail production injectors. These injectors were taken from light-duty diesel vehicles that are currently in operation on the UK roads and have done different mileages. All the production injectors suffered expulsions of ligaments and droplets after the end of injection (*a*EOI). It is shown that injector age/mileage has very little effect on the amount of expulsions compared to injection-to-injection variations in the amount of post-injection expulsions. Brand new production injectors also show the presence of these post-injection expulsions after every injection, which is not a desired feature of the modern solenoid actuated common-rail fuel injection system. Subsequent combustion of these post-injection ligaments and droplets lasted up to 25 ms after the end of fuel injection in our high pressure, high temperature experiments, and this would contribute to engine-out soot and unburned hydrocarbon (UBHC) emissions in a firing engine.

1. Introduction

In order to meet the current and future emission regulations, diesel engines are fitted with exhaust after treatment devices to reduce tail-pipe emissions of soot and NO_x. The load on these after treatment devices could be reduced if engine out NO_x, soot, and UBHC emissions could be better controlled. There is a greater need to understand the in-cylinder processes to further improve the fuel spray mixing processes and the accompanying combustion and emission formation. Much of the research is aimed at studying how combustion can be optimized, and emissions minimized, through optimizing fuel spray patterns and injection strategies [1–3], a recent example of research into the effect of end-of-injection rate shaping on combustion recession can be seen in [4]. Almost all of the studies, whether experimental or numerical, generally consider the spray behaviour from new injectors or injectors manufactured for research purposes. The research conducted by our group focusses on determining changes in the fuel spray evolution and how it degrades over time under normal on-road operation of production injectors. For the measurements done on injectors at different stages of their life cycle, expulsions of macroscopic fuel droplets and ligaments were observed directly *after* the end of injection. Similar observations were investigated earlier by other research groups [5–8], and the impact of the number of orifices on these expulsions was recently studied in [9]. Although these post-injection expulsions represent only a very small amount of fuel mass compared to the total fuel mass injected during a typical injection event, their sizes are larger compared to atomized droplets from the main injection which leads to sub-optimal burning conditions that increases the engine-out soot. Earlier research by Musculus et al. [10] has shown that sub-optimal mixture compositions can occur near the nozzle at the end of injection, and this

* Corresponding author at: HWLL103a, CEDPS Dept. of MACE, Brunel University London, Middlesex UB8 3PH, United Kingdom.
E-mail address: radboud.pos@brunel.ac.uk (R. Pos).

http://dx.doi.org/10.1016/j.fuel.2017.02.048
0016-2361/

can lead to an increase in unburned hydrocarbon engine-out emissions. In contrast to the current investigation, the research conducted in [10] focussed on low-temperature-combustion operation, and considered overly-lean mixture composition near the nozzle as a prime cause for UBHC.

In the present investigation the behaviour of post-injection expulsions from production injectors, and the impact of injector age (mileage) on these expulsions, have been studied. By looking subsequently at the combustion characteristics of droplets and ligaments, it becomes apparent that these post-injection expulsions can contribute to additional engine-out soot and UBHC emissions. A similar investigation on a smaller subset of injectors have been conducted in a non-reactive environment by the authors at an earlier stage, and this has been reported at the IMechE *Internal Combustion Engines* Conference [11]. The results presented here however treat a larger dataset along with the incorporation of combustion characteristics of post-injection expulsions as speculated in our earlier publication [11].

2. Experimental conditions

The measurements in this investigation were conducted in a constant volume chamber (CVC) under varying conditions to study different aspects of a fuel spray injection event. The main part of the experiment was conducted in a non-reactive, inert, low-temperature environment, to study droplet and ligament expulsions when there is no interference from combustion or evaporation. A subsequent study was conducted in a high-temperature engine-like environment to investigate expulsions under reactive conditions. Combustion of the main fuel injection event led to slight optical degradation of the expulsions, but combustion of ligaments and droplets after the main injection remained clearly visible. Based on our earlier experience with high-power LEDs in combination with CMOS-based high speed cameras [12], a front-lit configuration incorporating a green high-power LED, synchronized with a high speed camera and fuel injection equipment was applied. Fuel expulsions were recorded after the end of the main fuel injection event: Up to 0.7 ms *a*EOI under non-reactive conditions, and up to 25 ms *a*EOI under reactive conditions. In the subsequent sections the ambient conditions, injectors and injection conditions, and the recording conditions are treated in more detail. Table 1 provides a quick overview of the main experimental parameters, Fig. 1 provides a schematic of the set-up as applied in this research.

Table 1
Overview of the experimental parameters applied in this investigation.

Parameter	Setting
Injectors	6-Orifice nozzle, common-rail, solenoid actuated
Conditions	New(3), 30 k-mile(4), 63 k-mile(4), 92 k-mile(3)
Injection pressure	50.0 MPa (reactive), 80.0 MPa (non-reactive)
Duration	1.5 ms
Non-reactive ambient medium	Gaseous N_2, >99% purity
Pressure	3.30 MPa (±0.01)
Temperature	112 °C–118 °C
Image scale	77 µm/px
Image dimensions	39×39 mm^2, 512×512 px^2
Reactive, high *P-T* medium	Products of acetylene pre-combustion
Composition	approx. 11:77:8:4 O_2, N_2, CO_2, H_2O
Pressure	2.55 MPa (±0.04)
Temperature	930 K (±30)
Image scale	130 µm/px
Image dimensions	67×67 mm^2, 512×512 px^2
Recording frame rate	45 kfps
Frame time	22.2 µs
Illumination time	1.25 µs
LED illumination wavelength	521 nm
FWHM	40 nm
Duration	2.6 ms

2.1. Non-reactive ambient conditions

Inert, non-reactive measurements were made at 3.3 MPa back pressure in a medium of pure nitrogen, heated to a temperature of 112 °C–118 °C. By maintaining a low chamber temperature, rapid evaporation of expelled fuel droplets and ligaments was inhibited, which allowed us to image these expulsions over a prolonged time. By maintaining the system at a temperature above 110 °C, settling of diesel fuel on the windows post-injection was prevented, as any diesel film on the optical windows would degrade image quality of subsequent fuel injections. At a back pressure of 3.3 MPa the governing spray deceleration and breakup would be comparable to in-cylinder compression pressures of HSDI engines.

2.2. Reactive ambient conditions

Combustion measurements of post-injection expulsions were conducted at an ambient condition of 2.55 MPa at 900 K–960 K. The high temperature and pressure for the reactive conditions were achieved by pre-combustion of a lean acetylene mixture (volumetric air to acetylene ratio of 25:1) in the CVC at a starting pressure of 0.52 MPa and an approximate temperature of 320 K. Combustion of this lean mixture resulted in sufficient residual oxygen to ensure complete combustion of diesel fuel when subsequently injected into the CVC. The mixture composition of the ambient gas during diesel fuel injection, after pre-combustion, is provided in Table 1.

2.3. Injectors and injection conditions

The primary goal of this research was to investigate the degradation of diesel fuel spray characteristics resulting from normal on-road vehicle use. The injectors used in this investigation were acquired from vehicles that are operated on the UK roads. All of the used injectors were acquired from passenger cars, all same type, and were removed during standard maintenance at approximately 30, 60 and 90 thousand miles. The injectors were all still in working condition, and were solely removed to facilitate our research. The injectors were divided into four batches depending on the usage history:

- *New*: 3 new and unused injectors,
- *Set 1*: 4 injectors removed at 30,000 miles,

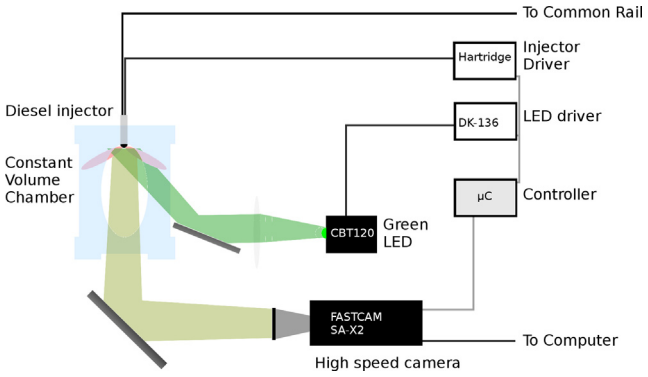

Fig. 1. Schematic of the experimental set-up as applied in this study.

- *Set 2*: 4 injectors removed at 63,000 miles which had received an after-market additive at 30,000 miles,
- *Set 3*: 3 injectors removed at 92,000 miles.

Each injector within a set came from the same engine, and all injectors were checked to have identical nozzle part numbers, ensuring same nozzle geometries. Before starting experiments, all injector nozzles were gently wiped with a dry tissue to remove loose deposits. Earlier experiments showed loose deposits would break off during injection in an inert environment, leading to particulates settling on the bottom window in the CVC. These in turn distorted images of subsequent recordings, as imaging was done through the bottom window. All used injector nozzles were discolored from deposits up to the sealing washer. Deposits on the *set 3* injectors were darker and thicker than *set 1* and *set 2* injector deposits. *Set 1* and *set 2* injectors showed no clear difference in deposit thickness or structure. It was therefore expected that *set 1* and *set 2* injectors would show similar droplet and ligament morphologies. *If* a difference would be seen when comparing expulsions from *new* injectors to those recorded from *set 1* or *2* injectors, it was expected the *set 3* injectors would show an even further increased effect. As will be shown, no difference in post-injection expulsions were however observed between the different sets of injectors.

Measurements were conducted at a common rail pressure of 80.0 MPa for the non-reactive measurements, and 50.0 MPa for the reactive measurements. The injection pressure was reduced for the reactive measurements to prevent wetting of the chamber walls, as reactive measurements were conducted at reduced ambient pressures and densities, resulting in both a higher initial spray tip velocity and a lower overall deceleration of the fuel spray. Condensation of diesel on the chamber windows did not occur as all diesel was burnt before the chamber temperature had decreased sufficiently to allow condensation of diesel vapour. For all investigations EN590 compliant commercial diesel was used as an injection fluid, and the injection duration was set at 1.5 ms to ensure the spray had attained a quasi steady-state spray shape.

2.4. High speed imaging

The fuel sprays were illuminated using a high-power green LED in a front lit configuration, where light back-scattered off the atomized stage of the injected fuel was collected by a high speed camera. Images were recorded to study the spray evolution from all six orifices simultaneously by looking head-on at the nozzle tip. In this configuration fuel vapour and vapour density gradients would be invisible. Sprays were recorded with a Photron FASTCAM SA-X2 high speed camera, set to record at 45 kfps, 512×512 px^2, and a shutter time of 1.25 μs. In the initial non-reactive recordings, a high magnification was applied, leading to a resolution of 77 μm/px and a total view screen of approximately 39×39 mm^2, as the detailed evolutions of droplet and ligament expulsions would be studied at their initial entrance into the chamber. For the subsequent reactive measurements a larger image window of 67×67 mm^2 was applied to follow droplets and ligaments over larger distances and over a longer time-scale. Although flame luminosity of the burning diesel spray and post-injection expulsions provided sufficient light to image the injection and combustion without application of an external light source, the LED was operated in an identical illumination mode as was applied in the inert measurements. This provided us both with a visible reference to directly relate the injection stages of the reactive and non-reactive conditions, and it also enhanced visibility of the fuel spray (especially post-injection ligaments) close to the nozzle, within the flame lift-off length, where initially no combustion was observed.

3. Results

At the ambient and injection conditions treated in the previous section, a total of 197 post-injection fuel expulsions, and their subsequent evolutions, were recorded. Fig. 2 shows the image streaks of evolving ligaments, where the leftmost image corresponds to the spray that was detected at EOI and all subsequent images were recorded at a time interval of 111 μs.

3.1. Non-reactive conditions

To determine the effect of injector age (mileage) on the quantity of ejected droplets and ligaments, spray measurements were carried out in an inert environment using two out of three new injectors and with all of the used injectors. Measurements of at least ten injection events were conducted per injector. Post-injection expulsions were observed for all injectors and they occurred in a random and non-reproducible way for every injection of all injectors. Orifice to orifice variations of the post-injection expulsions were large and the participating orifices too changed over time for subsequent injections. Fig. 3 provides (contrast-enhanced) images from subsequent recordings of a new injector, showing both large injection to injection variations and the change of participating orifices over time.

Images were analysed to extract the amount of visible fuel droplets and ligaments from post injection expulsions. As the actual droplet and ligament size lies at or below camera resolution, accurate quantitative determination of fuel mass/volume is impossible. A qualitative measurement of the amount of fuel expelled *a*EOI was determined in the form of camera pixel surface that covered the expelled liquid fuel. Although the determination was quantitative in nature, there is no conversion possible from observed liquid fuel area to actual ejected fuel mass. The quantitatively determined 'observed pixel coverage' are directly compared against each injector and injection, as the droplets and ligaments are expected to be similar in *actual* dimension and volume. Fig. 4 shows four post-injection images with accompanying analysis, one injection from each injector group. The first row shows the raw recorded image of the residual fuel spray after injection. The second row in Fig. 4 provides a magnified view of the central part of the image in the top row (red square), after application of several filters to enhance visibility of the expulsions. Third row provides a further filtering and amplification where ligaments and droplets (black dots) were identified by a selection algorithm, in order to determine the amount of pixels covered by the expulsions. Fourth row ultimately provides the original images with an overlay of detected droplets and ligaments (white). Red dots in the bottom row indicate algorithm-detected droplets that were rejected in a subsequent stage as being false-positives. Application of these filtering and determination steps to all recordings provided sufficient data to allow statistics with regard to average droplet expulsions and accompanying variations. As the contrast of expelled *a*EOI droplets and ligaments is low, discrimination between droplets/ligaments and residual atomized cloud is difficult, and the algorithm typically underestimated the actual amount of post-injection expelled fuel by 5%–15%. This was compensated for by combining subsequent frames of a post-injection expulsion to determine the average amount of ejected droplets. The algorithm also interpreted static specular reflections as droplets (depicted in the bottom row of Fig. 4 as red droplets). These falsely detected droplets were filtered out post-determination and were not included in subsequent analysis.

The results of the determined amount of post-injection expelled fuel is shown in Fig. 5, where every data point corresponds to the total amount of non-atomized fuel ejected after the end of

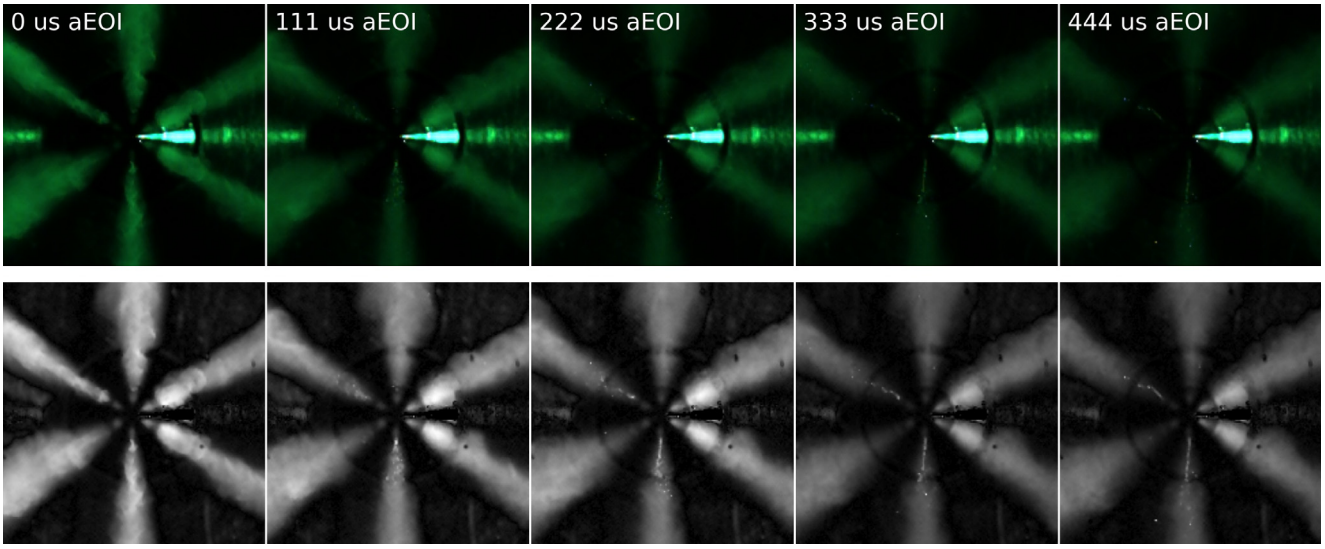

Fig. 2. Post-injection expulsions from a new injector. Leftmost image provides the end of the main injection, during needle drop. Subsequent images were recorded at indicated time *a*EOI, and show the evolution of post-injection ligaments emerging from the top-left and bottom orifices. Image size was 15×15 mm^2. Bottom row provides the same images, corrected for background artefacts, and recoloured to enhance visibility of expulsions.

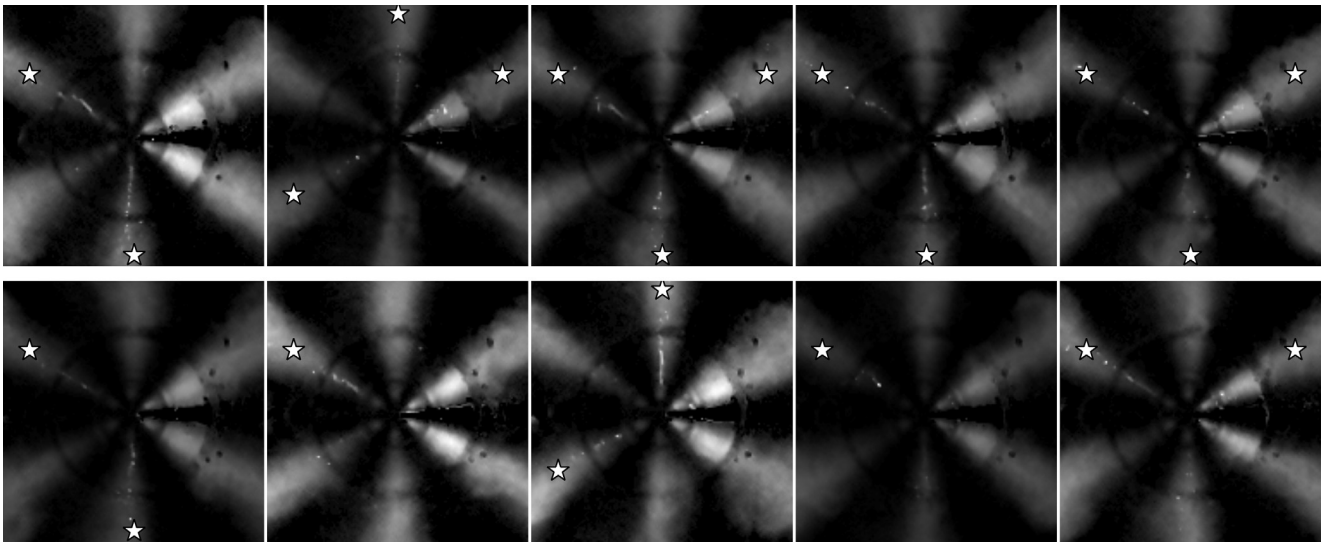

Fig. 3. Post-injection expulsions recorded from a new injector for ten successive injections. All images were recorded 0.51 ms *a*EOI and show the presence of expelled droplets and ligaments. White markers (stars) downstream of the sprays indicate which orifices clearly expelled fuel post-injection.

injection from the indicated injectors. As can be clearly seen in Fig. 5, the expelled mass from each injector show no clear trend from injection to injection, and all graphs randomly cross each other, providing no clearly visible differences between new and used injectors. The injection to injection variations of post-injection expulsions could be up to 250% for an individual injector, whilst the average ejected droplet surfaces for all injectors did not differ by more than 200%. The error bars in Fig. 5 provide a measure of the success rate of the algorithm to properly identify all ejected droplets and ligaments, and should therefore be treated as a systematic uncertainty of the algorithm rather than a fluctuation in the amount of ejected fuel.

As injection to injection repeatability of the amount of ejected droplets and ligaments was low, further analysis was done by considering the *variation* in determined expulsion surfaces. For each injector, a graph comparable to Fig. 5 was reduced to a single bar covering the interval within which all measured expulsion surfaces were contained, similar to the solid bars on the far-right in Fig. 5. In such a way, all expulsion variations could be combined into one graph to allow comparison of all injectors from new and used sets. Fig. 6 provides the resulting determined variation intervals, where every bar indicates the range over which determined post-injection expulsion surfaces are spread for ten injections, as shown in Fig. 5. For example a vertical bar ranging from 50 to 100 in Fig. 6 indicates that a given injector produced post-injection droplet expulsions of which the minimum amount of pixels covered by ligaments and droplets for all injections would cover 50 pixels, while in no recording post-injection expulsions covered more than a total of 100 pixels. For reference purposes, the numerical mean and standard deviation of the determined surfaces have been superimposed. All the determined ranges of total pixel counts for all injectors clearly overlap for the investigated ten injections per injector, without showing any clear increasing or decreasing trend in the amount of liquid fuel ejected post-injection. The two right-most datasets in Fig. 6 represent measurements from the *new* and *set 1* injectors acquired in an earlier investigation [11], where

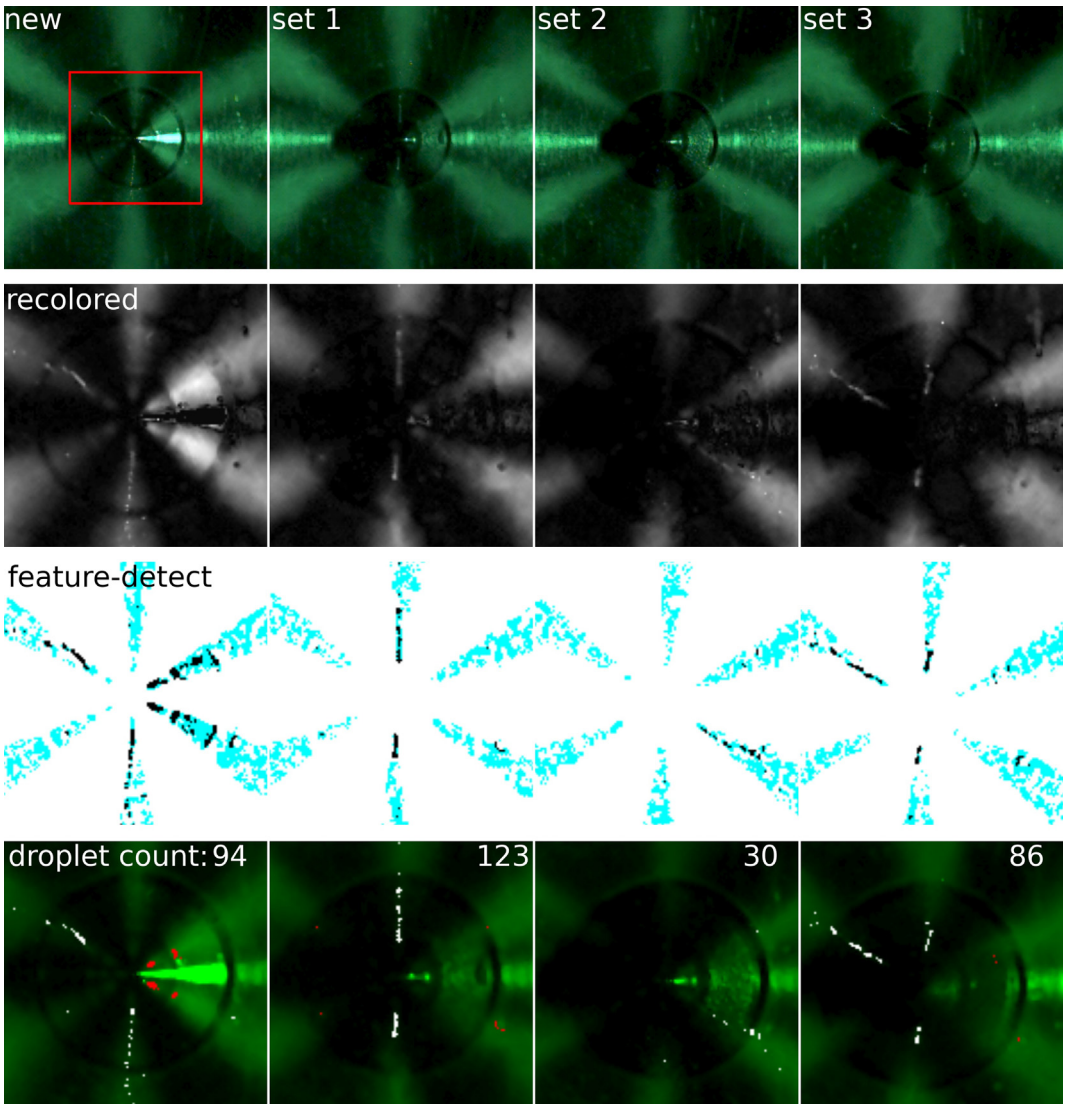

Fig. 4. Example analysis of one frame from a post-injection expulsion as recorded for four different injectors, at identical times *a*EOI. Numbers in the top-right corners of the bottom image rows indicate the total amount of pixels covered by ejected droplets and ligaments. An explanation of the images is provided in the text.

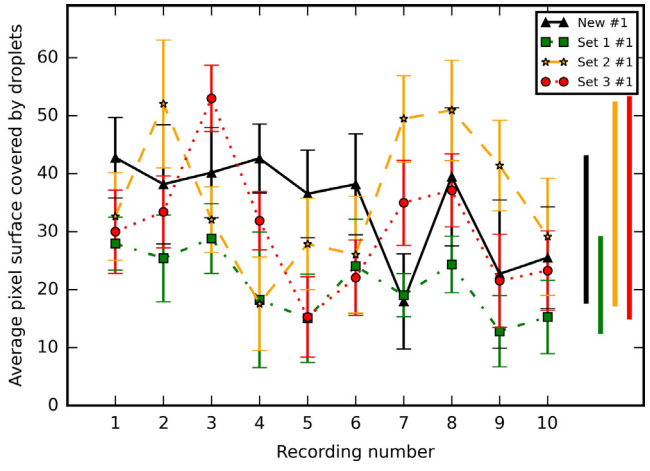

Fig. 5. Example of the lack of post-injection expulsion repeatability. Plotted are the determined amounts of droplets and ligaments, expressed in pixel counts, versus (chronological) recording number. Solid bars on the far right indicate the total range over which determined pixel surfaces varied for each injector.

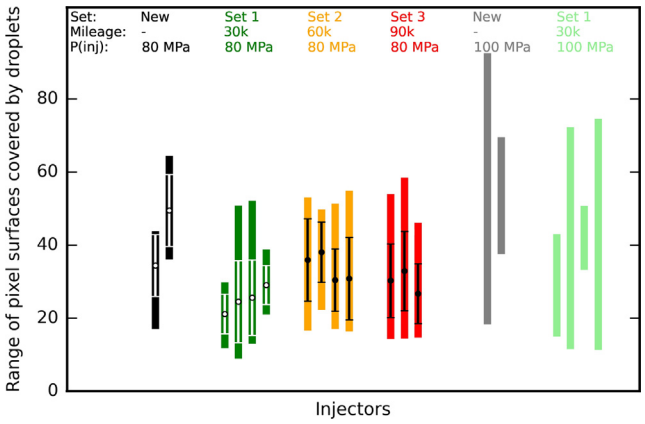

Fig. 6. Determined amount of droplet expulsions *a*EOI for every injector. Injector group (*new – set 3*) and corresponding injection pressures are provided above the two to four bars representing the individual injectors in every group.

injections were conducted at 100 MPa injection pressure. Based on the results so far, two important observations can be made:

- *All* injections from *all* injectors suffer from expulsion of droplets and ligaments *a*EOI. None of the interval bars provided in Fig. 6 touches the horizontal axis.
- Injector age has no observable effect on the ejected amount of droplets and ligaments for the injector mileage interval under consideration in this investigation. There is no trend visible in the positions of the bars in Fig. 6.

3.2. Reactive conditions

The relevance of the observed expulsions becomes apparent when the combustion characteristics of these droplets and ligaments are investigated. The *new* injector group consisted of three injectors, of which results of only two injectors have been treated up to this point. The third injector in this group was used for measuring post-injection expulsion behaviour under reactive conditions. As there was no observed difference between new and used injectors, moreover each injection of all injectors provided droplet expulsions, and as all expulsions showed large variations from injection to injection, there was no compelling reason to start an extensive measurement series on the burn characteristics of post injection expulsions for all injectors. Thus a few measurements are required under reactive conditions to acquire a qualitative understanding of the relevance of *a*EOI expulsion of droplets and ligaments, and only seven measurements were considered in this investigation. Combustion of the main injection event would provide sufficient illumination to properly record the spray flame, whilst the combination of the green LED would allow us to clearly discriminate between burning fuel and atomized/liquid stages of the injected spray, as the green light of the LED contrasts with the sooting, luminous, yellow flame. Fig. 7 provides a set of images from a reacting fuel injection event, where the leftmost image shows the spray flame prior to the end of injection and subsequent images were recorded at 111 μs intervals, comparable to the image streak provided in Fig. 2. Bottom row in Fig. 7 provides a detailed view of the centre 7×7 mm^2 of the corresponding images of the top row, providing a better view of the ligament formation near the tip of the nozzle.

Despite the high temperature conditions that the ligaments and droplets are ejected into, they clearly remain visible and maintain a *liquid* phase *a*EOI, and their evolution can be studied over a time frame of roughly 0.5 ms. Subsequent combustion of the evaporated atomised cloud close to the nozzle, originating from the main injection event, obscures the liquid expulsions from 0.5 ms *a*EOI onwards, masking out any subsequent breakup, evaporation, and start of combustion of the droplets and ligaments. The occurrence of the expulsions and their evolution provides the same characteristics as observed under inert conditions, and there is no observable difference in evolution of the post-injection expulsions when comparing inert and reactive conditions. Most notably, there is no clearly visible decrease in ligament and droplet size as a result of evaporation, and it is assumed that the effect of evaporation on the size of the droplets and ligaments lies below camera resolution. The observed rapid combustion of the injected fuel after the end of the main injection in combination with the subsequent prolonged burning of liquid fuel expelled *a*EOI, is expected to increase the temperature at the nozzle tip, and may cause additional deposit formation in the injector nozzle. Fig. 8 provides the evolution and combustion of atomized fuel, injected at the end of the main injection, followed by the ejection of ligaments and droplets *a*EOI. The less dense fuel spray from the main injection event appears to be weakly coupled to the injector orifices due to the lack of momentum, and can be seen to combust close to the nozzle tip. Burning droplets and ligaments continue to remain visible close to the nozzle tip well after the end of injection. The three blue dots in Fig. 8 correspond to the locations of three (out of six) orifices that produced post-injection expulsions.

4. Discussion

The large droplets and ligaments observed *a*EOI in this investigation are combusting at a much larger time scale, as their size negatively affects the evaporation rate. Fig. 9 shows a continued image streak of the combustion process that is visible in Fig. 7, clearly showing the persistence of burning droplets long after the main combustion event has ended. In the present investigation combustion in the CVC occurred in a slightly reduced-oxygen environment, however, the residual oxygen available during these experiments was certainly enough to burn all injected diesel.

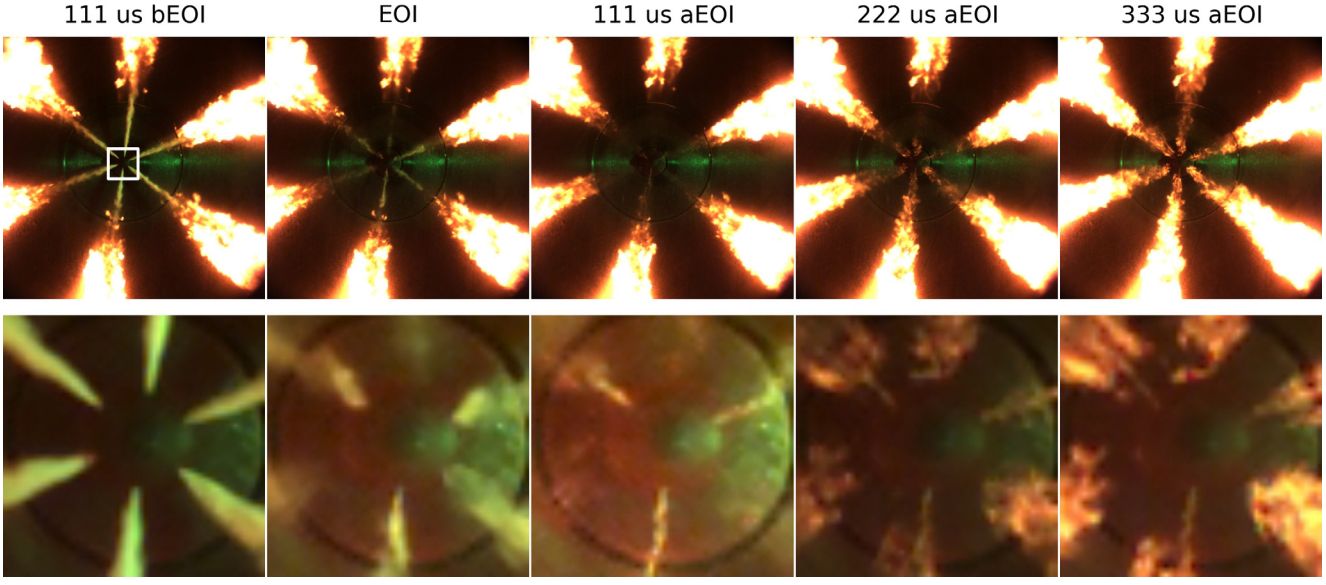

Fig. 7. End of injection and post-injection expulsions in a reactive environment, at indicated times before and after EOI. Image size is 67×67 mm^2. Bottom row shows the central 7×7 mm^2 of the top image row (white square in top-left image). Ligaments ejected from three orifices are visible as thin liquid streams in the bottom row, from the third frame onwards.

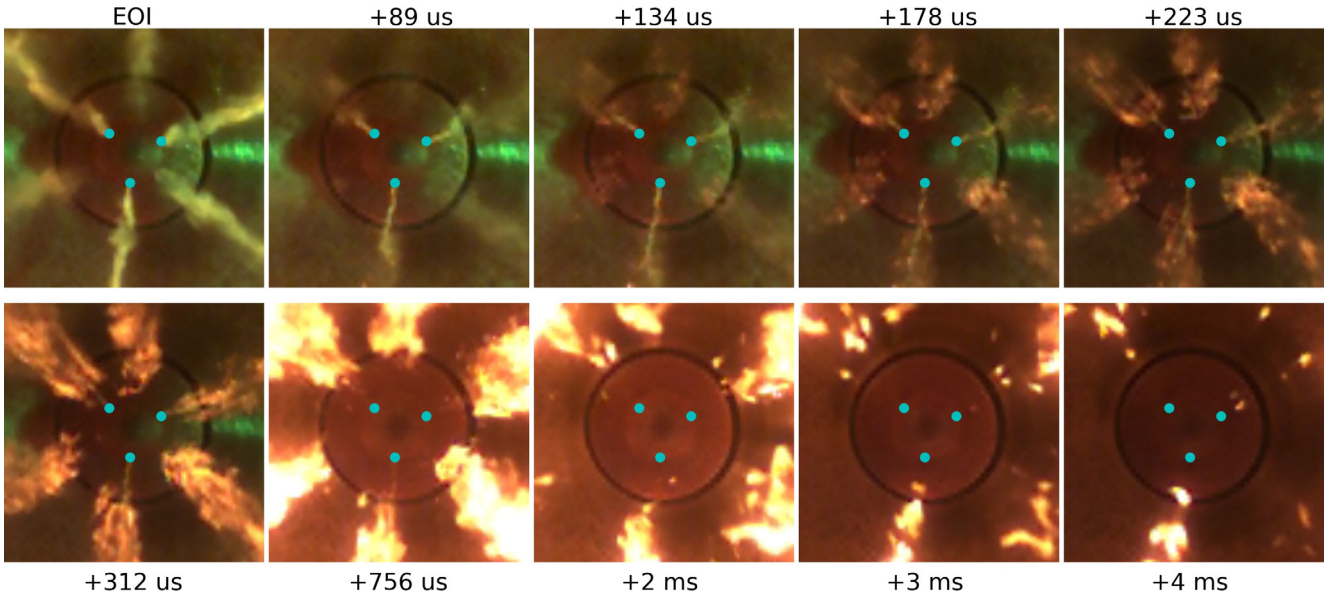

Fig. 8. Near nozzle *a*EOI spray evolution and subsequent combustion. The combustion flame of the main injection nearly touches the nozzle tip at 178 μs to 312 μs *a*EOI. Up to several milliseconds *a*EOI burning fuel droplets from post-injection expulsions remain close to the nozzle tip. Imaged area is 13×13 mm^2.

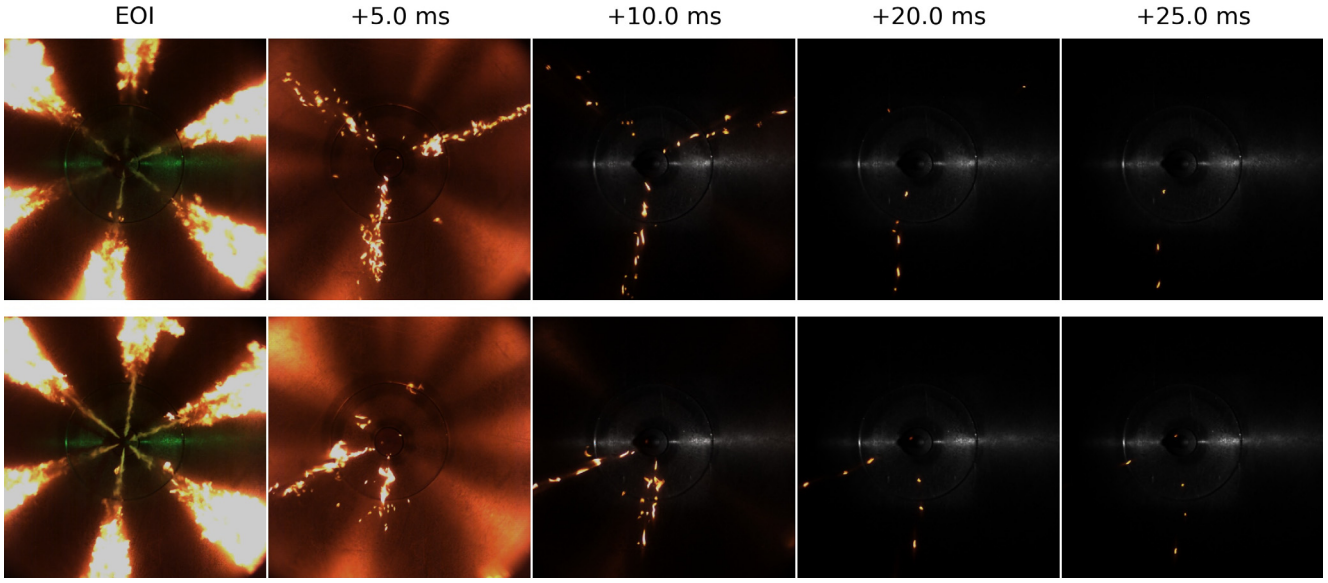

Fig. 9. (Top row) Continued combustion event provided in Fig. 7, where droplets remain visible long after the end of the main combustion. Leftmost image corresponds to the second image in Fig. 7. Subsequent images were recorded at 5, 10, 20 and 25 ms after EOI, which would correspond to 36°, 72°, 144° and 180° CAD *a*EOI for an engine speed of 1200 rpm. (Bottom row) Comparable combustion event and post-combustion expulsions burning from a second recording, recorded chronologically directly after the top-row recording.

Droplets and ligaments have been observed to burn up to 25 ms *a*EOI. The low ejection velocity of these post-injection expulsions might have reduced the entrainment rate, and a reduced local oxygen availability leads to slow continued oxidation. The expulsions observed in this work after the end of injection in the CVC will certainly occur in a production diesel engine. Depending on the fuel injection and ignition timings, expulsions of these ligaments and droplets could occur close to TDC position. The burn rate of this non-atomized liquid fuel may vary depending on the rich or lean operating regime prevailing inside the cylinder. For an engine speed of 1200 rpm the observed (prolonged) combustion of the droplets lasting up to 25 ms would correspond to 180° CAD. Due to reduced oxygen concentration after combustion and reduction in the cylinder temperature during the expansion stroke, the burning streaks of ligaments may be partially quenched, and it becomes apparent that these ejected ligaments and droplets may contribute to additional engine-out UBHC and soot. It is unfortunately not possible to determine if local quenching did occur in the experiments treated here. However it is certain that the expulsions that occurred *a*EOI continued to burn slowly, and this may contribute to additional engine out soot.

5. Conclusion

It has been shown in this investigation that droplets and ligaments are ejected after the end of diesel fuel injection, and this occurs for all recorded injections and for all investigated injectors

used in this research. Although injection to injection variation in the amount of fuel ejected after the end of injection is large, there is no visible trend indicating change over the lifetime of these injectors. As such, post-injection expulsions introduce a small quantity of non-atomized fuel *a*EOI into the engine cylinder, for new and used injectors irrespective of their age, and with a large injection to injection variation.

The combustion characteristics of these post-injection expulsions clearly indicate these droplets and ligaments may contribute to engine-out soot and UBHC emissions in production diesel engines.

Acknowledgements

This work was supported by Shell Global Solutions (UK) and the EPSRC, Grant No. EP/J018023/1.

References

[1] Tanaka T, Ando A, Ishizaka K. Study on pilot injection of di diesel engine using common-rail injection system. JSAE Rev 2002;23:297–302.
[2] Jung DW, Jeong JH, Lim OT, Pyo YD, Lee YJ, Iida N. Influence of pilot injection on combustion characteristics and emissions in a di diesel engine fueled with diesel and dme. SAE Technical Papers, 2011-01-1958; 2011.
[3] Pang KM, Ng HK, Gan S. Investigation of fuel injection pattern on soot formation and oxidation processes in a light-duty diesel engine using integrated cfd-reduced chemistry. Fuel 2012;96:404–18.
[4] Koci C, Martin G, Bazyn T, Morrison W, Svensson K, Gehrke C. The influence of diesel end-of-injection rate shape on combustion recession. SAE Int J Engines 2015;8(2):647–59.
[5] Kook S, Pickett LM, Musculus MPB. Influence of diesel injection parameters on end-of-injection liquid length recession. SAE Technical Papers, 2009-01-1356; 2009.
[6] Manin J, Bardi M, Pickett LM, Dahms RN, Oefelein JC. Microscopic investigation of the atomization and mixing processes of diesel sprays injected into high pressure and temperature environments. Fuel 2014;134:531–43.
[7] Kastengren A, Powell CF, Zak Tilocco F, Liu Z, Moon S, Zhang X, Gao J. End-of-injection behavior of diesel sprays measured with X-ray radiography. J Eng Gas Turbines Power 2012;134:094501–3.
[8] Swantek, AB, Duke D, Tilocco FZ, Sovis N, Powell CF, Kastengren AL. End of injection, mass expulsion behaviors in single hole diesel fuel injectors. ILASS, 26th Conference; 2014.
[9] Moon S, Huang W, Li Z, Wang J. End-of-injection fuel dribble of multi-hole diesel injector: comprehensive investigation of phenomenon and discussion on control strategy. Appl Energy 2016;179:7–16.
[10] Musculus MPB, Lachaux T, Pickett LM, Idicheria CA. End-of-injection over-mixing and unburned hydrocarbon emissions in low-temperature-combustion diesel engines. SAE Technical Papers, 2007-01-0907; 2007.
[11] Pos R, Cracknell R, Ganippa L. Characteristics of high pressure diesel sprays at the end of injection. IMechE ICE 2015, Conference Proceedings; 2015.
[12] Pos R, Cracknell R, Ganippa L. Transient characteristics of diesel sprays from a deposit rich injector. Fuel 2015;153:183–91.